

Leading Opinion

A double-chamber rotating bioreactor for the development of tissue-engineered hollow organs: From concept to clinical trial[☆]

M. Adelaide Asnaghi^{a,*}, Philipp Jungebluth^b, Manuela T. Raimondi^{c,d}, Sally C. Dickinson^e, Louisa E.N. Rees^f, Tetsuhiko Go^b, Tristan A. Cogan^f, Amanda Dodson^f, Pier Paolo Parnigotto^g, Anthony P. Hollander^e, Martin A. Birchall^h, Maria Teresa Conconi^g, Paolo Macchiarini^b, Sara Mantero^{a,*}

^a Department of Bioengineering, Politecnico di Milano, Piazza Leonardo da Vinci 32, 20133 Milan, Italy

^b Department of General Thoracic Surgery, Hospital Clinic de Barcelona, University of Barcelona, c Villarroel 170, E-08036 Barcelona, Spain

^c LaBS, Department of Structural Engineering, Politecnico di Milano, Piazza Leonardo da Vinci 32, 20133 Milan, Italy

^d IRCCS Galeazzi Orthopaedic Institute, Via R. Galeazzi 4, 20161 Milan, Italy

^e Department of Cellular and Molecular Medicine, University of Bristol, School of Medical Sciences, University Walk, Bristol BS8 1TD, UK

^f School of Clinical Veterinary Science, University of Bristol, Langford, Bristol BS40 5DU, UK

^g Department of Pharmaceutical Sciences, University of Padua, Via F. Marzolo 5, 35131 Padua, Italy

^h Department of Clinical Medicine at South Bristol, Faculty of Medicine and Dentistry, University of Bristol, Bristol, UK

ARTICLE INFO

Article history:

Received 22 June 2009

Accepted 10 July 2009

Available online 3 August 2009

Keywords:

Bioreactor

Tissue engineering

Co-culture

Oxygenation

Stem cells

Airway transplantation

ABSTRACT

Cell and tissue engineering are now being translated into clinical organ replacement, offering alternatives to fight morbidity, organ shortages and ethico-social problems associated with allotransplantation. Central to the recent first successful use of stem cells to create an organ replacement in man was our development of a bioreactor environment. Critical design features were the abilities to drive the growth of two different cell types, to support 3D maturation, to maintain biomechanical and biological properties and to provide appropriate hydrodynamic stimuli and adequate mass transport. An analytical model was developed and applied to predict oxygen profiles in the bioreactor-cultured organ construct and in the culture media, comparing representative culture configurations and operating conditions. Autologous respiratory epithelial cells and mesenchymal stem cells (BMSCs, then differentiated into chondrocytes) were isolated, characterized and expanded. Both cell types were seeded and cultured onto a decellularized human donor tracheal matrix within the bioreactor. One year post-operatively, graft and patient are healthy, and biopsies confirm angiogenesis, viable epithelial cells and chondrocytes. Our rotating double-chamber bioreactor permits the efficient repopulation of a decellularized human matrix, a concept that can be applied clinically, as demonstrated by the successful tracheal transplantation.

© 2009 Elsevier Ltd. All rights reserved.

1. Introduction

There are many clinical situations in which it would be desirable to replace hollow organs, such as airways, bowel and bladder, with functional substitutes, and where conventional means of reconstr-

uction are inadequate. Recently, there has been growing optimism that cell-, including stem cell-, based tissue-engineering methods may effectively replace the structure and function of these organs, and there have been early clinical successes with bladder [1] and, most recently, trachea [2]. Although bioreactors have played a central role in tissue engineering for two decades [3,4], this new need to sustain the diverse requirements of complex organ constructs demands a correspondingly intelligent bioreactor environment.

The trachea is an ideal model for early clinical translation of bioreactor-based tissue-engineering technology: it is a relatively simple conduit without intrinsic motility and there is a clear clinical need for large airway grafts [5,6]. A clinically applicable tracheal substitute must meet numerous requirements: an external hyaline cartilage framework and an internal epithelial covering are

[☆] *Editor's Note.* This paper is one of a newly instituted series of scientific articles that provide evidence-based scientific opinions on topical and important issues in biomaterials science. They have some features of an invited editorial but are based on scientific facts, and some features of a review paper, without attempting to be comprehensive. These papers have been commissioned by the Editor-in-Chief and reviewed for factual, scientific content by referees.

* Corresponding authors. Tel.: +39 02 2399 3376; fax: +39 02 2399 3360.

E-mail addresses: adelaide.asnaghi@mail.polimi.it (M.A. Asnaghi), sara.mantero@polimi.it (S. Mantero).

essential [5,7,8]. Although there are reports of small volumes tracheal cartilage generation and clinical application [9–14], progress with long segment grafts has been limited by lack of an ideal scaffold, well-established epithelial and chondrocyte culture techniques, and an appropriate bioreactor environment.

Key requirements of a tracheal bioreactor are (a) the provision of different culture conditions on either side of the organ wall, and (b) the need for adequate mass transport of gases and nutrients within a construct that has to be more than 4 cm long to be clinically useful [5]. Based on these criteria, we developed a step-wise work plan consisting of the following: design of a bioreactor, development of predictive analytical models, *in vitro* testing, *in vivo* trials in animal model, application of human cells and performance of a first-time-in-man transplantation of the resultant recellularized construct.

2. Materials and methods

2.1. Bioreactor design

Objectives of the bioreactor design were: (1) to facilitate cell seeding procedures on both sides of a 3D tubular matrix, ensuring homogeneous plating; (2) to allow seeding and culturing of different cell types on either side of the tubular scaffold; (3) to enhance oxygenation of the culture medium and mass transport (oxygen, nutrients and catabolites) between the medium and the adhering cells; (4) to stimulate the cells with hydrodynamic stimuli, favoring the metabolic activity and the differentiation process; (5) to allow the achievement and maintenance of sterility and other criteria of Good Laboratory Practice (GLP), simplicity and convenience and (6) to permit the possibility of automation and scale-up/-out. Thus, a rotating double-chamber bioreactor was designed: the device allows confined seeding and culturing on both surfaces of a tubular matrix and includes rotatory movement of the scaffold around its longitudinal axis. By immersing half of the construct in media at any one moment, cells are cyclically exposed to gaseous (incubator atmosphere) and liquid (medium) phases. During exposure to the incubator atmosphere, the construct remains wet and the thin surface layers of culture medium are oxygen-saturated cyclically (Fig. 1).

The device has three main components: culture chamber, motion and control units. A polymeric culture chamber houses the biologic sample and the medium for the whole culture period. Cylindrical scaffold holders were constructed with working ends from 10 to 25 mm in diameter – to house matrices of different dimensions – and a central portion of smaller diameter to expose the luminal surface of the matrix for seeding and culturing. Once the biological construct is in place, the inner space is confined (inner chamber) and isolated from the rest of the

culture environment (outer chamber) by the graft wall. A co-axial conduit links the inner chamber to the external environment through an appropriate interface at the chamber wall which provides access to seed and feed the luminal surface of the construct. A luer-lock Hepa filter is connected to the conduit to preserve oxygenation and sterility. Secondary elements moving with the scaffold holder induce continuous mixing of the culture medium to increase its oxygenation and the exchange of nutrients and catabolites. The chamber is closed by a Petri-like cover to permit both oxygenation and sterility of the culture environment. The intact system can be autoclaved, significantly reducing contamination risks. The cell/matrix construct is moved by a DC motor (0–5 rpm adjustable) separated from the culture compartments. The connection between the motion unit and the culture chamber allows the first to remain in the incubator for the whole culture period, moving the chamber independently every time is needed (i.e. sampling, medium exchange). An external control unit regulates and monitors rotation. At the end of the culture period, rotation is turned off, both chambers are emptied and refilled with fresh media and the bioreactor used to convey the graft to the operating theatre.

2.2. Oxygenation

A crucial consideration was whether it would be theoretically feasible to support the oxygenation needs of a large, cellular organ construct within a rotating bioreactor. To explore this fundamental question, a mathematical model was developed and used to predict oxygen concentration profiles in tissue constructs of a clinically relevant thickness (1 mm), with varying oxygen consumption rate, colonization depth, and density of cells. Transport of oxygen in the construct was described by the mass conservation law in diffusion reaction

$$\frac{\partial c}{\partial t} = D\nabla^2 c - V \quad (1)$$

where c is the molar concentration, D is the diffusivity coefficient through the construct, V is the molar rate of consumption per unit volume.

The following assumptions were made. The profiles were calculated in stationary state. A cylindrical symmetry was assumed, using the hypothesis of infinite length, such that one-dimensional profiles were calculated within the construct thickness. The tissue thickness was modelled in three distinct regions (Fig. 2): region 1, facing the inner bioreactor chamber, populated with epithelial cells, region 2 facing the outer bioreactor chamber, populated with chondrocytes, and region 3, acellular, in between. Rates of oxygen consumption, V , were determined as the product of maximal mammalian cells consumption rate, V_{\max} , and cell volume density, N_v

$$V = V_{\max} \cdot N_v \quad (2)$$

The following boundary conditions were assumed. The axial rotation allows both internal and external construct surfaces to remain in contact with oxygen-

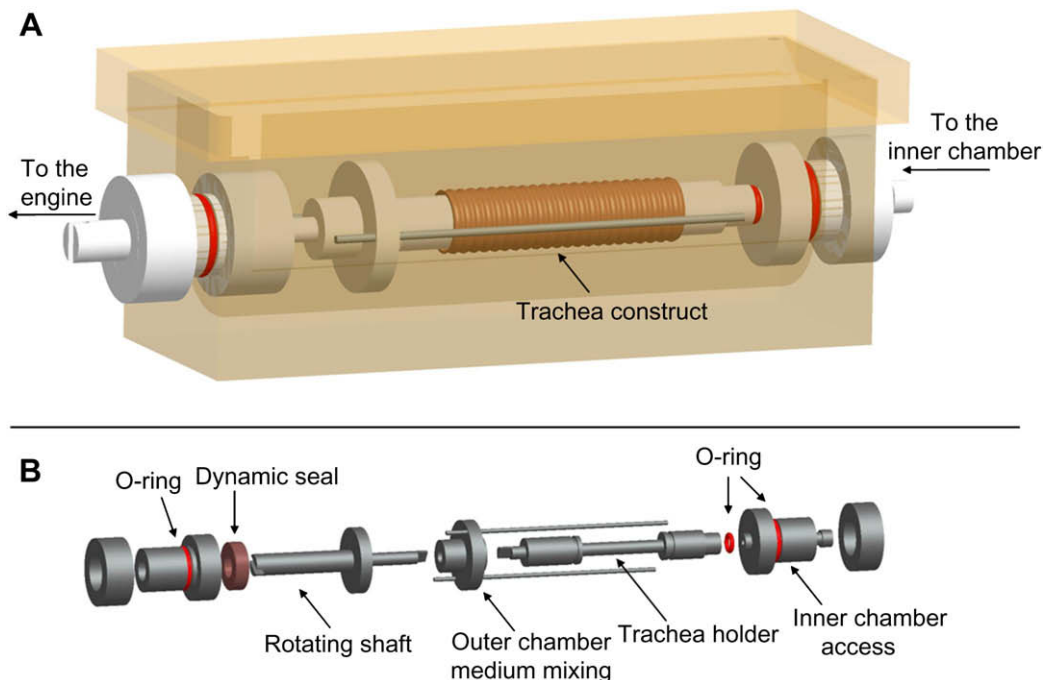


Fig. 1. Three-dimensional view of the bioreactor assembly (A) and exploded view of its components (B).

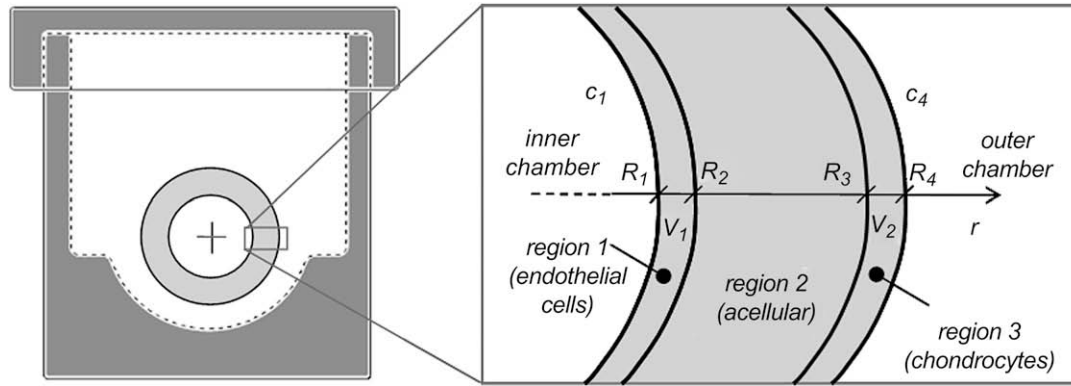


Fig. 2. Subdivision scheme of the trachea tissue construct in cross section, assumed for the modelling prediction of oxygen concentration in the tissue and in the media during bioreactor culture. The tissue is subdivided in 3 regions: region 1 facing the inner bioreactor chamber, populated with epithelial cells, region 2 acellular, and region 3 facing the outer bioreactor chamber, populated with chondrocytes. V – cell oxygen consumption rate; $R_2 - R_1$ – thickness of the region populated by endothelial cells; $R_4 - R_3$ – thickness of the region populated by chondrocytes; c_1 – inner bioreactor chamber oxygen concentration; c_4 – outer bioreactor chamber oxygen concentration.

saturated films of medium. Thus, the liquid-phase oxygen concentration at the construct surfaces was assigned the value of the equilibrium concentration for oxygen in the media, calculated using Henry's law constant for O_2 in water at 37 °C (Table 1). The concentration profiles and the oxygen fluxes were assumed to be continuous at all interfaces between regions.

Solving Eq. (1) yielded the oxygen concentration profile through the tissue in each thickness region

$$c(r) = c_1 + \frac{V_1}{4D}(r^2 - R_1^2) + a \quad (3)$$

$$c(r) = c_1 + \frac{V_1}{4D}(R_2^2 - R_1^2) + \frac{V_1 R_2^2}{2D} \ln \frac{r}{R_2} + a \quad (4)$$

$$c(r) = c_4 + \frac{V_2}{4D}(r^2 - R_4^2) + \frac{1}{2D} \ln \frac{r}{R_4} (V_1 R_2^2 - V_2 R_3^2) + a \quad (5)$$

for $R_1 < r < R_2$, $R_2 < r < R_3$, and $R_3 < r < R_4$, respectively, where

$$a = \frac{\ln \frac{r}{R_1}}{\ln \frac{R_4}{R_1}} \left\{ c_4 - c_1 + \frac{1}{2D} \left[V_1 R_2^2 \ln \frac{R_2}{R_4} + V_2 R_3^2 \ln \frac{R_4}{R_3} + \frac{V_2}{2} (R_3^2 - R_4^2) + \frac{V_1}{2} (R_1^2 - R_2^2) \right] \right\}. \quad (6)$$

The parameter values used in the calculations are given in Table 1. To determine the effect of specific parameters on the profiles, the parameters were varied and the profiles recalculated. To evaluate the effect of cell invasion, the two regions populated with cells were assumed of three thickness values, equal on both cell-populated regions: 125, 250 and 500 μm . For each thickness value, the oxygen profile was calculated at four values of increasing cell volume density: 20×10^6 , 40×10^6 , 60×10^6 and 80×10^6 cells/mL.

A second mathematical model was implemented and used to predict oxygen concentration drop in the culture media during those periods when the bioreactor rotation is turned off (for example during construct transfer to the surgical room). Again, transport of oxygen was described by the mass conservation law in diffusion reaction (Eq. (1)), with new assumptions and boundary conditions.

The diffusion term was neglected, in the hypothesis of well mixed medium. Michaelis–Menten kinetics was assumed for the uptake of oxygen by cells, V

$$\frac{dc}{dt} = -V(c) = -V \frac{c}{K_m + c} \quad (7)$$

where K_m is the Michaelis–Menten constant. Oxygen uptake was assumed to be linear at very low concentrations and it was expressed in total moles

$$\frac{dc}{dt} \cdot V_m = -V \cdot \frac{c}{K_m} \cdot V_t \quad (8)$$

where V_m and V_t are the chamber priming volume and the tissue volume, respectively. For both chambers, the initial condition assumed was 20% oxygen partial pressure and the final condition was a critical 1% partial pressure. Solving Eq. (8) yielded the expression of the time, t_{cr} , in which the critical oxygen concentration is reached

$$t_{cr} = \left(-\frac{K_m \cdot V_m}{V \cdot V_t} \right) \cdot \ln 0.05. \quad (9)$$

The parameter values assumed for calculation of t_{cr} are given in Table 1. To determine the effect of specific parameters on t_{cr} , the parameters were varied and the critical times recalculated, as described above for the oxygen profiles.

2.3. Bone marrow stem cell (BMSC) culture and characterisation

BMSCs were isolated and cultured as previously reported [2]. Plastic-adherent mesenchymal BMSCs were expanded until 90% confluent, in the presence of 5 ng/mL basic fibroblast growth factor (PeproTech, London, UK), before being passaged and re-plated at 1×10^6 cells per 175 cm^2 flask.

Prior to differentiation and subsequent implantation into the patient, the stem cell characteristics and differentiation potential of the BMSC population were assessed. Phenotypic cell surface markers present on passage 3 cells were analysed by fluorescence-activated cell sorting (FACS) as previously described [19]. Positive expression was defined as the level of fluorescence greater than 98% of the isotype control.

The multi-lineage differentiation potential of the passage 3 BMSCs was assessed by examining their osteogenic, adipogenic and chondrogenic capacities. BMSCs were grown in monolayer culture for 3 weeks in the presence of osteogenic differentiation medium, containing dexamethasone, ascorbic acid 2-phosphate and

Table 1
Model parameters used to predict oxygen concentration profiles in a trachea tissue construct cultured in a double-chamber rotating bioreactor, and to predict oxygen concentration in the culture media filling the chambers with bioreactor rotation turned off.

Parameter	Inner	Outer
O_2 solubility in water at 37 °C [nmol/mL/mmHg]		1.3 [15]
Tissue construct wall thickness, $R_4 - R_1$ [mm]		1
O_2 diffusion coefficient in H_2O at 37 °C, D [cm^2/s]		2.1×10^{-5} [15]
O_2 consumption rate, V_{max} [$\mu\text{mol}/10^6$ cells/h]	0.2027 [16]	0.108 [17]
Boundary O_2 concentration in culture [mM]	0.195	0.195
Boundary O_2 concentration post-implant [mM]	0.195	0.05
Thickness of the cell-populated region [μm]		30 (validation culture), 125, 250, 500 (parametric study)
Construct cell volume density, N_v [10^6 cells/mL]		20, 40, 60, 80 (parametric study)
Construct cell volume density, N_v [10^6 cells/mL]	41.25 (validation culture)	61.33 (validation culture)
Chamber priming volume, V_m [mL]	10	120
Michaelis–Menten constant, K_m [mM]		0.15 [18]

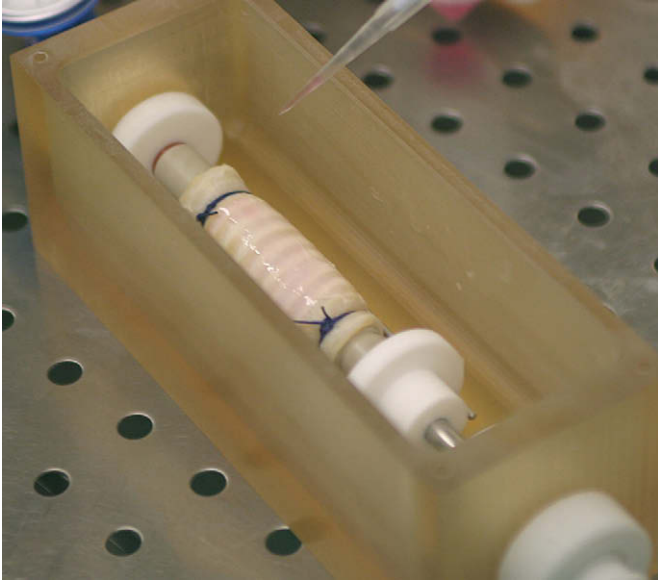


Fig. 3. The matrix inside the bioreactor during the seeding process.

β -glycerol phosphate (R&D Systems, Abingdon, UK), and minerals deposited by stimulated cells were stained with 40 mM alizarin red (Fluka). BMSCs were also grown for 3 weeks in adipogenic differentiation medium, containing hydrocortisone, isobutylmethylxanthine and indomethacin (R&D Systems), and fat vacuoles in the stimulated cells were stained with fresh oil red-O solution. For chondrogenic differentiation, BMSCs were seeded onto fibronectin-coated polyglycolic acid (PGA) scaffolds and cultured on a gently rotating platform for 35 days in medium containing insulin–transferrin–selenium (Invitrogen), TGF- β 3 (R&D Systems), dexamethasone and ascorbic acid 2-phosphate (Sigma), according to our previously published method [20]. Biochemical assays were used to measure the amounts of various proteins in the tissue-engineered cartilage constructs. As previously described, proteoglycan was measured by colorimetric assay, total collagen by amino acid analysis and collagen types I and II by specific ELISA assays [21].

Having verified the stem cell characteristics of the BMSC population, passage 3 cells were induced to differentiate into chondrocytes, as previously described [2], prior to seeding onto the decellularised donor scaffold using our bioreactor.

2.4. Respiratory epithelial cells culture

Respiratory epithelial cells were isolated and cultured as previously reported [22]. Briefly, bronchoscopic biopsy samples were placed in 70% ethanol for 30 s and then in a solution containing 0.25% trypsin (Sigma–Aldrich), 100 U/mL penicillin and 100 μ g/mL streptomycin in PBS in a centrifuge tube overnight at 4 °C. At 24 h, we

warmed the tissue to 37 °C for 45 min and then disrupted it by repeated vigorous pipetting with a plugged glass Pasteur pipette. We neutralised the trypsin solution with complete medium (Dulbecco's modified Eagle's medium [DMEM], Invitrogen, Paisley, UK), containing 10% fetal calf serum (PAA, Yeovil, UK), penicillin (100 U/mL), and streptomycin (100 μ g/mL). We repeated the dissociation process, and centrifuged the cell suspension at 1000 revolutions per min for 10 min. We resuspended the cell pellet in keratinocyte serum-free medium (Invitrogen), supplemented with 25 μ g/mL bovine pituitary extract, 0.4 ng/mL recombinant epidermal growth factor, 0.06 mmol/L calcium chloride, 100 U/mL penicillin and 100 μ g/mL streptomycin, seeded the cells in a final volume of 5 mL in 25 cm² flasks, and incubated the cultures at 37 °C, 5% CO₂ for 2–3 days for adherence. Culture medium was then replaced every 5 days. Cytospins of cultured autologous recipient epithelial cells at first passage were subjected to three-colour immunofluorescence histology for cytokeratins 5 and 8, type I collagen and counterstained with DAPI to confirm epithelial phenotype before attachment to the matrix in the bioreactor. Ten fields of view were examined per slide, equating to a minimum of 250 cells.

2.5. Human tracheal decellularization

A 7 cm tracheal segment was retrieved from a transplant donor and rinsed in phosphate buffered saline (PBS) containing 1% penicillin, 1% streptomycin, and 1% amphotericin B (all Sigma, Barcelona, Spain), having removed all loose connective tissue. 25 cycles of the decellularization protocol as previously reported were applied [2,23,24]: tissue was extensively washed with distilled water for 72 h, then incubated in 4% sodium deoxycholate and 2000 kU deoxyribonuclease I in 1 mmol/L sodium chloride (Sigma Chemicals, Barcelona, Spain). The presence of cellular elements and MHC-positive cells was verified by immunohistochemistry after each cycle. Primary anti-human HLA-D (BD Biosciences, Oxford, UK) and HLA-ABC (Abcam, Cambridge, UK), secondary antibodies (Vectastain ABC kit, Vector Laboratories), and a peroxidase substrate kit (DAB, Vector Laboratories) were used to detect MHC antigen expression. For negative controls, we omitted the primary antibody. Paraffin-embedded sections of the matrix were also stained with 4'-6-diamidino-2-phenylindole (DAPI, Vector Laboratories, Burlingame, CA, USA) to detect residual nuclei inside the treated tissue. Samples of the treated matrix were fixed with 3% glutaraldehyde (Merk, Darmstadt, Germany) in 0.1 M cacodylate buffer (Prolabo, Paris, France), subjected to critical point drying and gold sputtering, and examined by scanning electron microscope (JSM6490, JEOL, Japan).

2.6. Bioreactor cultivation of the trachea construct

Both cell seeding onto the scaffold and cellularized construct dynamic culture were performed inside the bioreactor, avoiding construct manipulation between the two operations and thus limiting the risk of cell construct contamination. The acellular matrix was positioned onto the cylindrical holder, fixed at both ends with surgical sutures to ensure rotation and positioned inside the bioreactor. The recipient's cultured cells were detached from culture flasks, diluted with medium (1×10^6 cells per mL), and seeded onto the matrix. Chondrocytes were dropped longitudinally on the external surface of the matrix with a microsyringe, while epithelial cells were injected onto the internal surface (Fig. 3). After completion of the seeding process, each chamber was filled up with their respective complete media to totally submerge the seeded matrix. The resultant cellularized construct was maintained in static conditions for 24 h to promote cell adhesion (37 °C, 5% CO₂). Media volumes were then reduced so that nearly half of the matrix was

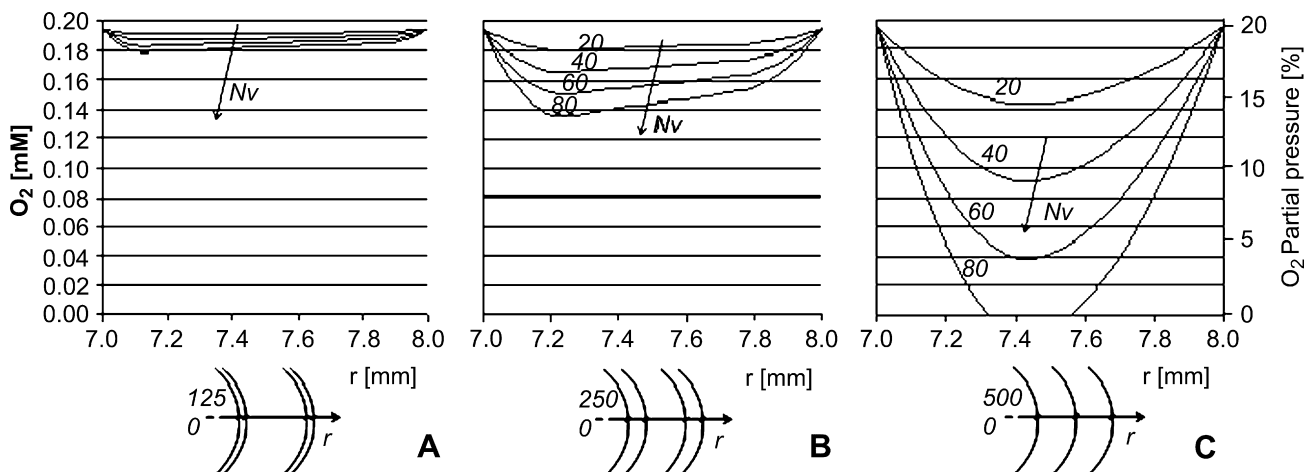


Fig. 4. Model predictions of oxygen concentration profiles plotted on the cross section of the trachea tissue construct during rotating bioreactor culture. The plots refer to a cell-populated thickness of (A) 125 μ m, (B) 250 μ m, and (C) 500 μ m. The various curves refer to different cell densities, N_v , expressed in 10^6 cells/cm³.

Table 2

Prediction of maximum allowable time, t_{cr} , before a 95% drop in oxygen concentration is reached in the culture media filling the bioreactor chambers with bioreactor rotation turned off.

Cell density [10^6 cells/cm ³] (parametric study)	t_{cr} [h], inner chamber			t_{cr} [h], outer chamber		
	125 μ m	250 μ m	500 μ m	125 μ m	250 μ m	500 μ m
20	3.6	1.8	0.9	69.2	34.3	16.9
40	1.8	0.9	0.4	34.6	17.2	8.4
60	1.2	0.6	0.3	23.1	11.4	5.6
80	0.9	0.4	0.2	17.3	8.6	4.2
Validation culture	30 μ m			30 μ m		
41.2 (inner), 61.3 (outer)	7.4			83.2		

exposed to the incubator atmosphere (75 mL external, 4 mL internal) and dynamic culture was started at 1.5 revolutions per min (37 °C, 5% CO₂) for 72 h. The external medium (chondrocytes) was changed every 48 h and the internal medium (epithelial cells) every 24 h. At the end of the culture period, the bioreactor rotation was turned off, both chambers were emptied and completely refilled with fresh media and the bioreactor was delivered to the operating room. The graft was then cut to shape and implanted into the patient as a replacement for her left main bronchus. Ethical permission was obtained from the Spanish Transplantation Authority and the Ethics Committee of the Hospital Clinic, Barcelona.

Predictions of the concentration profile within the tissue construct were obtained from Eqs. (3) to (6), in two conditions: during bioreactor culture and post-implantation. The parameter values used for all calculations relevant to bioreactor validation are gathered in Table 1. In both conditions, the thickness of both the cell-populated regions was assumed equal to 30 μ m, based on measurements taken on histological sections of the construct. In the implanted condition, at the construct inner surface oxygen was set at 20% partial pressure whereas at the construct outer surface it was assigned a 5% partial pressure value, corresponding to venous blood oxygen tension, 38 mmHg. The critical time in which oxygen partial pressure in the medium drops to 1% in the absence of bioreactor rotation, t_{cr} , was calculated for both chambers using Eq. (9).

2.7. Imaging

Sections of graft surplus to clinical need were fixed with 3% glutaraldehyde (Merk, Darmstadt, Germany) in 0.1 M cacodylate buffer (Prolabo, Paris, France),

subjected to critical point drying and gold sputtering, and analysed by scanning electron microscopy (JSM6490, JEOL, Japan) to qualitatively evaluate cell adhesion and proliferation on the matrix preimplantation.

Immediately prior to implantation, the internal surface of the graft was brushed, and again by bronchoscopy at two weeks, as previously reported [2]. At two months, biopsies of the graft wall were taken by flexible bronchoscopy under topical anaesthesia and sedation. Specimens were embedded in OCT (Sakura, CA), snap-frozen and mounted on cork disks in isopentane cooled over liquid nitrogen, and stored at –80 °C. Five micrometer frozen tissue sections were cut on a cryostat (Bright, Huntingdon) and processed for haematoxylin and eosin histology and multiple colour immunofluorescence, as previously described [2,25]. Sections were air dried and fixed for 10 min in ice-cold acetone before blocking for 1 h with 5% human and goat serum. Samples were then incubated at 4 °C overnight with optimally titrated primary monoclonal antibodies in two combinations. Stain 1 consisted of mouse anti-human monoclonal antibody to collagen II (Abcam) to confirm the presence of chondrocytes, an anti-human monoclonal antibody to cytokeratins 5 and 8 (BD Biosciences) to identify epithelial cells, and stained for nuclear DNA with DAPI. Stain 2 used the same antibody to cytokeratins 5 and 8 (BD Biosciences) plus an anti-human HLA-DR, DP, DQ (PharMingen) to identify MHC class II positive cells (antigen-presenting cells and vascular endothelium). Sections were washed in PBS and incubated for 1 h at room temperature with goat anti-mouse isotype-specific secondary fluorochrome conjugates (Southern Biotechnology Associates Inc, USA). Where necessary, a three-stage procedure used biotinylated isotype-specific secondary antibodies followed by AMCA Avidin D (Vector Laboratories Inc, USA). Sections were mounted with Vectashield® (Vector laboratories Inc, USA) and sealed with nail varnish. Multiple fields at 20 \times magnification were digitized and grey scale images captured on a Leica DMRA microscope using a Hamamatsu Orca-ER camera and Q-Fluoro software (Leica, UK).

3. Results

3.1. Oxygenation

Modelling predictions of oxygen profiles in the trachea tissue construct during rotating bioreactor culture are presented in Fig. 4. Oxygen concentration in the tissue decreases for increasing colonization depth and density of cells. At a cell-colonised depth of 125 μ m on both tissue sides, oxygen concentration is maintained above 0.18 mm (18.5% partial pressure or 138 mmHg) at all cell

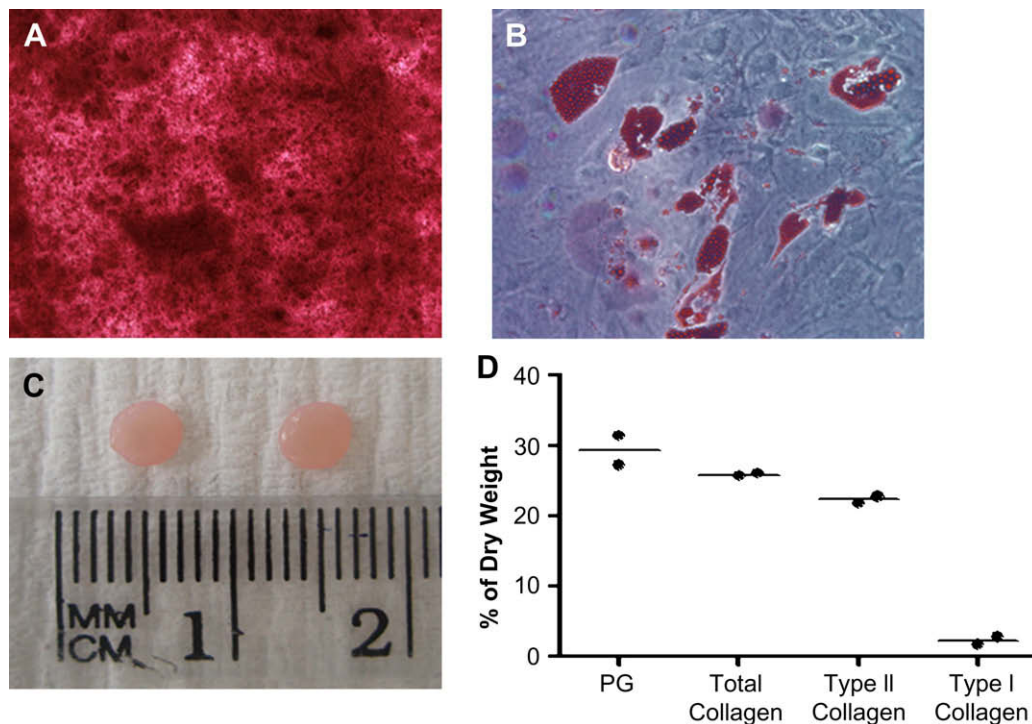


Fig. 5. Multi-lineage differentiation potential of BMSCs. Expanded BMSCs from passage 3 were incubated in osteogenic or adipogenic differentiation medium for 3 weeks. Minerals characteristic of osteogenic differentiation were stained with alizarin red (A) and fat vacuoles characteristic of adipocytes were stained with oil red-O (B). Photographs are shown at 10 \times magnification. BMSCs were seeded onto PGA scaffolds and cultured in chondrogenic differentiation medium for 35 days. The macroscopic appearance of duplicate tissue-engineered cartilage constructs is shown in (C) and the biochemical analysis of the protein content of the constructs is shown in (D) (PG = proteoglycan).

densities. At cell-colonised depths of 500 μm on both tissue sides, corresponding to a full-thickness cell invasion, oxygen concentration drops to a minimum level of 0.04 mm (4.1% partial pressure or 31 mmHg) at a cell density of 60×10^6 cells/cm³, while zero concentration values are predicted in the internal regions of the construct at 80×10^6 cells/cm³.

Modelling predictions of the critical time in which a 95% drop in oxygen concentration is reached in the media filling the static bioreactor chambers are given in Table 2. The critical time decreases for increasing cell-colonised depths and cell densities. Values range from around 4 h to 13 min and from 70 to 4 h, in the internal and external bioreactor chambers respectively.

3.2. Characterisation of BMSC population

BMSCs were isolated from an autologous bone marrow aspirate by their ability to adhere to tissue culture plastic. The cells were allowed to proliferate until a sufficient number were obtained for

seeding onto the decellularised donor trachea. Prior to seeding, passage 3 BMSCs were characterized to assess the quality of the stem cell preparation.

FACS analysis was used to assess the population for phenotypic cell surface markers associated with multipotent stem cells. In agreement with previously published results [19], the population was positive for CD105 (99.3%), STRO-1 (30.5%), VCAM-1A (28.3%), CD49a (25.8%), bone morphogenetic protein receptor 1A (1.9%) and CD117 (1.3%). As expected the cells were negative for CD34, a haematopoietic stem cell marker.

The multi-lineage differentiation potential of the BMSCs was assessed by examining their chondrogenic, osteogenic and adipogenic capacities. The BMSC population was successfully differentiated into both osteoblasts, resulting in cultures rich in minerals, and adipocytes, as shown by the presence of fat vacuoles stained with oil red-O (Fig. 5A and B). In addition, a white, shiny tissue resembling hyaline cartilage at the macroscopic level was generated when BMSCs were seeded onto PGA scaffolds and cultured in

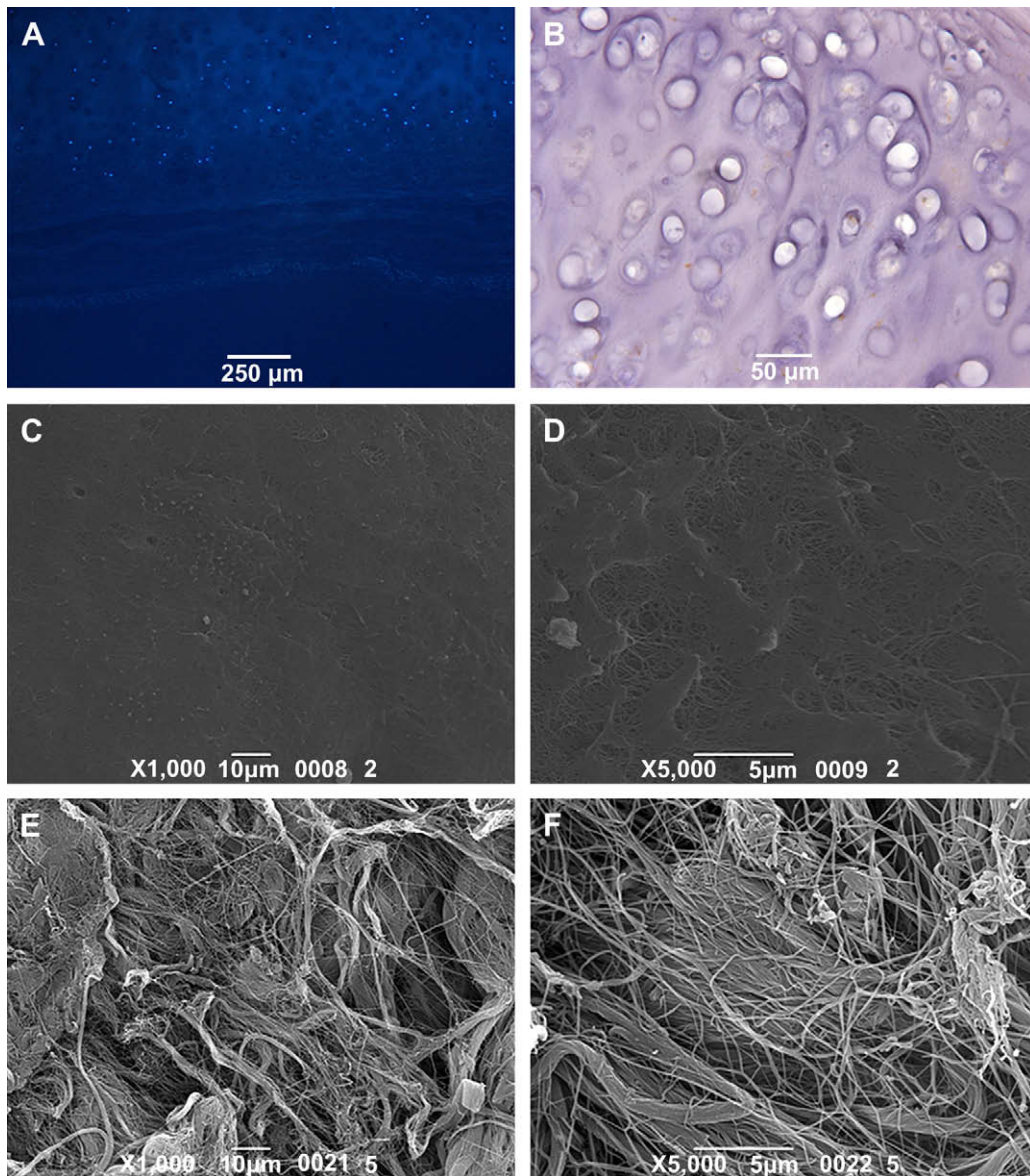


Fig. 6. Tracheal matrix after 25 cycles of the detergent-enzymatic treatment. As revealed by DAPI staining (A; 50 \times), only few nuclei were still present inside the cartilage rings. A mild immunoreactivity against HLA-DR, HLA-DP, HLA-DQ antigens was visible in small areas (B; 200 \times). Interruptions of the basal lamina characterized the luminal surface (C, D), whereas an irregular network of collagen fibers were present on the external one (E, F).

chondrogenic differentiation medium for 35 days (Fig. 5C). When duplicate tissue-engineered cartilage constructs were analysed for several matrix proteins, amounts of proteoglycan and type II collagen, the two major constituents of adult hyaline cartilage, were similar to previously published results [20]. Levels of type I collagen, which is virtually absent in normal, mature hyaline cartilage, were minimal (Fig. 5D).

Having shown that the BMSC population displayed cell surface marker and multipotential characteristics of stem cells, passage 3 cells were induced to differentiate into chondrocytes by stimulating with TGF- β 3, dexamethasone and insulin in the presence of parathyroid hormone-related peptide to inhibit hypertrophy [2,20]. The cells were then seeded onto the outer surface of the decellularised donor trachea using our bioreactor.

3.3. Respiratory epithelial cells culture

All cells in epithelial culture stained positive for cytokeratins 5 and 8 immediately before seeding and had epithelial morphology on light microscopy of cultured cells. We did not detect any fibroblasts morphologically or by immunofluorescence histology looking for cells positive for type I collagen. As at least 250 cells were examined per slide, this represents greater than 99.6% purity of the epithelial cell culture.

3.4. Human trachea decellularization

After 25 cycles of decellularization, epithelial and glandular cells were completely removed from the tracheal matrix, while only a few chondrocytes were still visible (Fig. 6A). Treated tissue was free from HLA-A, HLA-B, and HLA-C antigens, although low amounts of focal MHC class II expression were still seen in a few areas (Fig. 6B). High magnification of the luminal surface revealed that the basal lamina was partially maintained (Fig. 6C and D). Indeed, an alternation of smooth areas and matrix fibers was well visible. The external side of tracheal matrix was characterized by bundles of fibers irregularly arranged (Fig. 6E and F).

3.5. Bioreactor cultivation of the trachea construct

The procedure described to seed chondrogenic BMSCs and epithelial cells on either side of a long tubular tracheal matrix allowed easy and highly efficient cell seeding. The bioreactor worked properly and no contamination was observed during the whole culture period. Autoclavability, ease of handling under sterile conditions, reliability and precision ensured full compatibility of the device with the GLP rules.

Modelling predictions of oxygen profiles in the tracheal tissue construct during rotating bioreactor culture and post-implantation are presented in Fig. 7. Oxygen in the tissue is maintained at 20% partial pressure during culture and ranges linearly from 20% to 5% partial pressure (38 mmHg) after implantation. The critical time in which a 95% oxygen drop is reached in the media filling the static bioreactor chambers was around 7 h for the inner chamber and 83 h for the outer chamber (Table 2). Therefore, a maximum time of 7 h was available to safely deliver the construct to the operating room and maintain it in static conditions until the time of implant.

3.6. Graft outcomes

As previously reported [2], brushings of the graft immediately before implantation showed that both cell types remained in significant numbers and were viable, confirmed by scanning electron microscopy analysis of the graft surplus (Fig. 8). This was also the case two days post-implantation [2]. At two months, graft

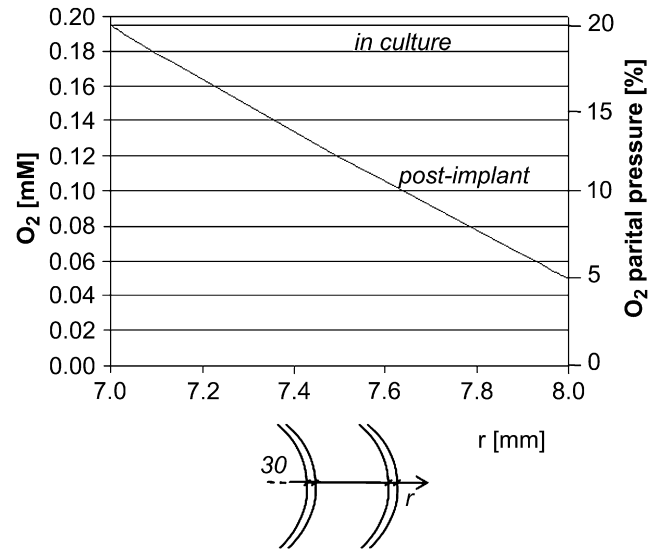


Fig. 7. Model predictions of oxygen concentration profiles plotted on the section of the trachea tissue construct during bioreactor validation culture and in the post-implantation condition.

biopsy showed vigorous angiogenesis and remodeling (Fig. 9). Immunofluorescence histology confirmed the presence of angiogenesis and showed reconstitution of epithelium, the continued presence of viable chondrocytes, and a reappearance of the mucosal lymphoid cells that typically densely populate normal tracheal mucosa [26]. Results of the recipient's lung function tests are as high at one year as they were at 4 months [2]. She is fully active and well, and caring for her two children.

4. Discussion

In response to the need to replace pathological hollow organs, bioengineered products offer potential advantages over conventional treatments or allografts. Solutions using autologous cells, whether primary or stem cell-derived, offer functional restoration without the need for immunosuppression. Cells can be obtained from small biopsies, expanded and differentiated as necessary with

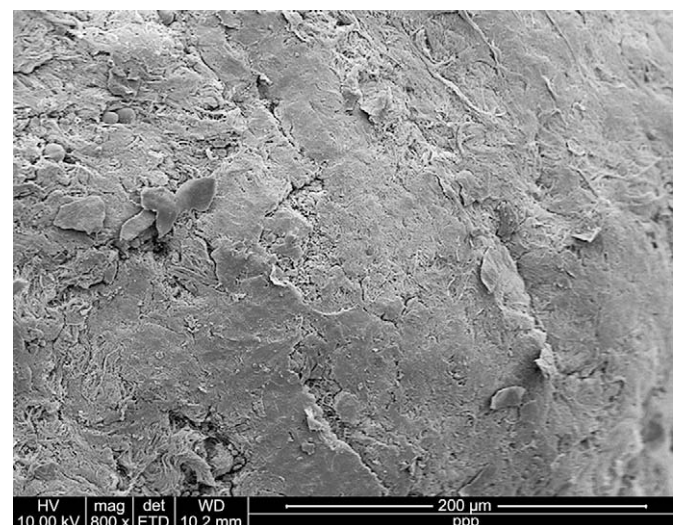


Fig. 8. Scanning electron microscopy image of the outer surface of the graft surplus to clinical need, showing a continuous layer of adherent cells.

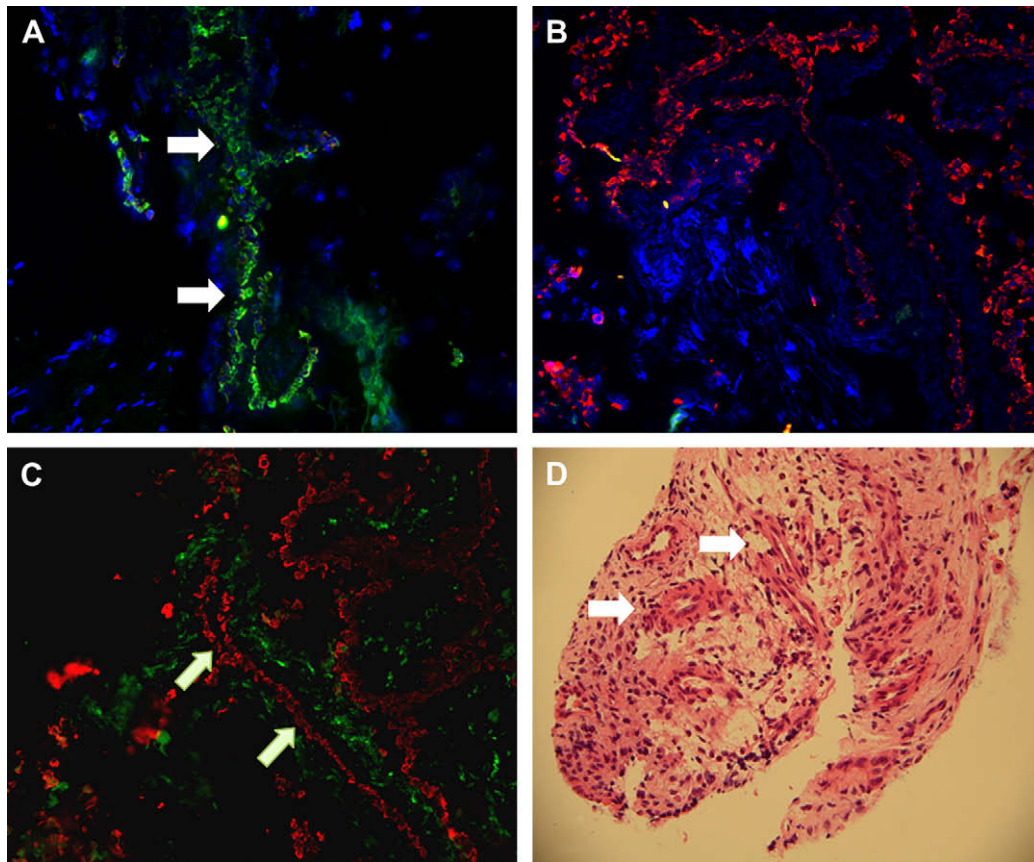


Fig. 9. Histology of graft biopsies taken by bronchoscopy two months after implantation in a patient. Superficial section (A) and deep section (B) three-colour immunofluorescence histology (20 \times): green, cytokeratins 5 and 8; red, collagen II; blue, DAPI (nuclei). A sheet of viable epithelial cells (green) is shown in (A) (arrows), and many viable chondrocytes (red) are shown in (B). Two-colour immunofluorescence histology (C; 20 \times) showing epithelial cells (green), MHC class II (red: antigen-presenting cells, endothelium). The epithelium (green) is already associated with a well-developed microvasculature (arrows, red). Haematoxylin and eosin image of deep biopsy (D; 20 \times) showing early revascularization (arrows).

high yield and purity. Starting with tissues such as skin [27], and moving onto more complex hollow organs including more than one cell type, such as bladder [1] and trachea [2], tissue-engineered constructs, populated with autologous-derived cells, are showing promising results in early clinical trials. However, as structure and function becomes more complicated, the *in vitro* culture environment assumes an increasingly important role. It is necessary to address the diverse demands of more than one cell type, whilst increasing construct size raises serious questions about the ability of the environment to deliver adequate oxygen concentrations to all cells.

Bioreactors have been designed to provide solutions to a wide range of questions relating to cell and tissue engineering. Altering bioreactor microenvironments, adding control of medium flow and mixing, may guide structural and functional properties of tissues [28–30]. Mechanical cues may be introduced to stimulate cells to produce specific components [31–33], or align cells in specific functionally relevant ways [34,35]. As the goal of such research is to produce clinically useful products, bioreactors can also provide quality-assured and cost-effective manufacturing processes, with full compliance to relevant regulatory frameworks and the possibility of smooth scale-up/-out through automation and robotics. In this context, the present article focuses on the design and development of a bioreactor for long tubular construct engineering that allows double seeding and culturing on both the inner and the outer surface of the matrix.

Thanks to the ultrastructure of biological acellular trachea matrices, two separate chambers are obtained inside and outside

the tubular scaffold, and the two cell types can be fed with their proper culture medium. When using permeable porous scaffolds, the great advantage of double seeding from both the inner and the outer surface of a matrix in our double-chamber bioreactor results in a much better cell colonization throughout the scaffold thickness (unpublished data), overcoming another generally limiting aspect of traditional static culture techniques. Moreover, the bioreactor rotates the construct around its longitudinal axis providing proper oxygenation to the three-dimensional structure and improves mass transport between the culture media and the adhering cells.

Gradients of oxygen and nutrients exist in engineered tissue, due to the balance between transport and rates of cellular consumption. Due to the difficulty of monitoring these gradients within tissue [36], predictive mathematical models have been developed for various bioreactor-cultured tissues, such as cardiac muscle [37], bone [38,39] and cartilage [40–42]. Oxygen is the focus of most of these models, due to its limited solubility in aqueous media. In this context, to further validate the bioreactor design, we explored the feasibility of providing adequate oxygenation to cells within a thick scaffold by using a mathematical transport model. This was used to predict oxygen concentration in the bioreactor-cultured trachea construct and in the culture media, as a function of construct geometry, thickness of cell invasion into the scaffold wall, cell densities and oxygen consumption rates. The model is designed to compare representative culture configurations and operating conditions of the rotating bioreactor. The consumption rates assumed here, 0.1 and

0.2 $\mu\text{mol}/10^6$ cells/h, were in the range previously reported for primary cells in culture, 0.1–0.5 $\mu\text{mol}/10^6$ cells/h [15]. In the construct, the assumption that cells consumed oxygen uniformly at a zero-order rate was found to be an overestimate. Indeed, our model predictions demonstrated that oxygen concentrations do not fall to critical values at any time under a wide range of operating conditions. These data provide important validation of the rotating bioreactor as an adequate environment for the development of thick-walled, cellular, tissue-engineered hollow organ implants. Compared to previously derived finite element models [37,40,41], our analytical model was conceived in a parametric form, in order to single out critical bioreactor operating conditions, such as the culture of full-thickness cell-populated constructs at very high cell densities.

Currently, the major limitation of our rotating bioreactor is the low level of automation of the system. An automatic medium conditioning and exchange system is desirable in order to minimize contamination risks and protect homeostasis. This would operate unattended over a period of days or weeks, whilst permitting intermittent, sterile evaluation of pH, nutrient or waste concentration. A system controller would also be useful to manage the tissue-engineering process. Monitoring the data provided by sensors, allied to closed loop feedback, will allow more control and, thereby, reproducibility of expansion, differentiation and migration of cells within the scaffold.

The most innovative outcome of our work lies in the fact that using the developed bioreactor we made possible to properly re-personalise a donor trachea and to successfully perform the first engineered airway transplantation without the need of any immunosuppressive therapies. The graft is still functioning well and there is no sign of rejection at one year post-implantation. Cytological and histological studies were necessarily limited by the need to avoid trauma to the graft. However, we have confirmed vigorous angiogenesis, by laser Doppler recordings from two weeks, and at biopsy at two months.

We have also confirmed the persistence of viable chondrocytes, and a layer of viable epithelial cells at two months post-surgery. However, the epithelial layer, whilst macroscopically intact and clearing mucus by this time, was microscopically discontinuous. Thus, further work to improve epithelial cell coverage of the internal surface of the graft pre-operatively is necessary, and this is an important design consideration for further refinements of the bioreactor. Furthermore, we hypothesize that the application of flow stimuli to the internal compartment of the bioreactor will encourage appropriate alignment and function of cilia prior to implantation, thereby initiating appropriate clearance of mucus from the first post-operative day.

5. Conclusions

Following mathematical modelling of hypothetical cellular oxygen requirements, we designed a double-chamber bioreactor to support hollow organ (tracheal) recellularized implants. We confirmed that the bioreactor configuration allowed oxygenation to be maintained despite the thickness of the implant wall, and that two autologous cell types with disparate media requirements could be supported, expanded and would migrate effectively on the scaffold. Ultimate validation of the bioreactor's effectiveness was provided by its central role in the first stem cell-derived, tissue-engineered organ, which continues to function well ten months post-implantation. Further refinements will be necessary to permit scale-up and full clinical trials, as well to explore hypothetical ways of improving graft production, such as encouraging angiogenesis and orientated ciliary function.

Acknowledgements

This work was done with grant support from the Ministero dell'Istruzione, dell'Università e della Ricerca, Italy, the Ministerio de Sanidad y Consumo, Instituto de Salud Carlos III, Fondo de Investigación Sanitaria (FIS) (PI050987), Spain, the Charles Courtenay-Cowlin Fund, University of Bristol, UK (Dr. Rees), the UK Arthritis Research Campaign (APH) and the James Tudor Foundation (SCD). Thanks go to Dr. Simon Rose, Pathology Department, Royal United Hospital Bath NHS Trust for haematoxylin and eosin studies of human implant tissue post-operatively.

References

- [1] Atala A, Bauer SB, Soker S, Yoo JJ, Retik AB. Tissue-engineered autologous bladders for patients needing cystoplasty. *Lancet* 2006;367:1241–6.
- [2] Macchiarini P, Jungebluth P, Go T, Asnaghi MA, Rees LE, Cogan TA, et al. Clinical transplantation of a tissue-engineered airway. *Lancet* 2008;372:2023–30.
- [3] Martin I, Wendt D, Heberer M. The role of bioreactors in tissue engineering. *Trends Biotechnol* 2004;22:80–6.
- [4] Wendt D, Riboldi SA, Cioffi M, Martin I. Bioreactors in tissue engineering: scientific challenges and clinical perspectives. *Adv Biochem Eng Biotechnol* 2009;112:1–27.
- [5] Grillo HC. Tracheal replacement: a critical review. *Ann Thorac Surg* 2002;73:1995–2004.
- [6] Macchiarini P. Trachea-guided generation: deja vu all over again? *J Thorac Cardiovasc Surg* 2004;128:14–6.
- [7] Macchiarini P. Tracheal transplantation: beyond the replacement of a simple conduit. *Eur J Cardiothorac Surg* 1998;14:621–3.
- [8] Walles T. Bioartificial tracheal grafts: can tissue engineering keep its promise? *Expert Rev Med Devices* 2004;1:241–50.
- [9] Osada H, Takeuchi S, Kojima K, Yamate N. The first step of experimental study on hybrid trachea: use of cultured fibroblasts with artificial matrix. *J Cardiovasc Surg (Torino)* 1994;35:165–8.
- [10] Macchiarini P, Walles T, Biancosino C, Mertsching H. First human transplantation of a bioengineered airway tissue. *J Thorac Cardiovasc Surg* 2004;128:638–41.
- [11] Kim J, Suh SW, Shin JY, Kim JH, Choi YS, Kim H. Replacement of a tracheal defect with a tissue-engineered prosthesis: early results from animal experiments. *J Thorac Cardiovasc Surg* 2004;128:124–9.
- [12] Kojima K, Vacanti CA. Generation of a tissue-engineered tracheal equivalent. *Biotechnol Appl Biochem* 2004;39:257–62.
- [13] Walles T, Giere B, Hofmann M, Schanz J, Hofmann F, Mertsching H, et al. Experimental generation of a tissue-engineered functional and vascularized trachea. *J Thorac Cardiovasc Surg* 2004;128:900–6.
- [14] Wu W, Cheng X, Zhao Y, Chen F, Feng X, Mao T. Tissue engineering of trachea-like cartilage grafts by using chondrocyte macroaggregate: experimental study in rabbits. *Artif Organs* 2007;31:826–34.
- [15] Palsson BO, Bhatia SN. Scaling up for ex vivo cultivation. In: *Tissue engineering*. Upper Saddle River, NJ: Pearson-Prentice Hall; 2004. p. 223–43.
- [16] Kondo M, Tamaoki J, Sakai A, Kameyama S, Kanoh S, Konno K. Increased oxidative metabolism in cow tracheal epithelial cells cultured at air–liquid interface. *Am J Respir Cell Mol Biol* 1997;16(1):62–8.
- [17] Godara P, McFarland CD, Nordon RE. Design of bioreactors for mesenchymal stem cell tissue engineering. *J Chem Technol Biotechnol* 2008;83:408–20.
- [18] Galbusera F, Cioffi M, Raimondi MT, Pietrabissa R. Computational modeling of combined cell population dynamics and oxygen transport in engineered tissue subject to interstitial perfusion. *Comput Methods Biomech Biomed Engin* 2007;10(4):279–87.
- [19] Kafienah W, Mistry S, Williams C, Hollander AP. Nucleostemin is a marker of proliferating stromal stem cells in adult human bone marrow. *Stem Cells* 2006;24:1113–20.
- [20] Kafienah W, Mistry S, Dickinson SC, Sims TJ, Learmonth I, Hollander AP. Three-dimensional cartilage tissue engineering using adult stem cells from osteoarthritis patients. *Arthritis Rheum* 2007;56:177–87.
- [21] Dickinson SC, Sims TJ, Pittarello L, Soranzo C, Pavesio A, Hollander AP. Quantitative outcome measures of cartilage repair in patients treated by tissue engineering. *Tissue Eng* 2005;11:277–87.
- [22] Rees LE, Gunasekaran S, Sipaul F, Birchall MA, Bailey M. The isolation and characterisation of primary human laryngeal epithelial cells. *Mol Immunol* 2006;43:725–30.
- [23] Conconi MT, De Coppi P, Di Liddo R, Vigolo S, Zanon GF, Parnigotto PP, et al. Tracheal matrices, obtained by a detergent-enzymatic method, support in vitro the adhesion of chondrocytes and tracheal epithelial cells. *Transpl Int* 2005;18:727–34.
- [24] Jungebluth P, Go T, Asnaghi MA, Bellini S, Martorell J, Calore C, et al. Structural and morphological evaluation of a new detergent-enzymatic tissue engineered tracheal tubular matrix. *J Thorac Cardiovasc Surg*, in press.

- [25] Rees LE, Pazmany L, Gutowska-Owsiak D, Inman CF, Phillips A, Stokes CR, et al. The mucosal immune response to laryngopharyngeal reflux. *Am J Respir Crit Care Med* 2008;177(11):1187–93.
- [26] Barker E, Haverson K, Stokes CR, Birchall M, Bailey M. The larynx as an immunological organ: immunological architecture in the pig as a large animal model. *Clin Exp Immunol* 2006;143:6–14.
- [27] Priya SG, Jungvid H, Kumar A. Skin tissue engineering for tissue repair and regeneration. *Tissue Eng Part B Rev* 2008;14:105–18.
- [28] Lichtenberg A, Tudorache I, Cebotari S, Ringes-Lichtenberg S, Sturz G, Hoeffler K, et al. In vitro re-endothelialization of detergent decellularized heart valves under simulated physiological dynamic conditions. *Biomaterials* 2006;27:4221–9.
- [29] Radisic M, Marsano A, Maidhof R, Wang Y, Vunjak-Novakovic G. Cardiac tissue engineering using perfusion bioreactor systems. *Nat Protoc* 2008;3:719–38.
- [30] Arrigoni C, Chitto A, Mantero S, Remuzzi A. Rotating versus perfusion bioreactor for the culture of engineered vascular constructs based on hyaluronic acid. *Biotechnol Bioeng* 2008;100:988–97.
- [31] Kim BS, Nikolovski J, Bonadio J, Mooney DJ. Cyclic mechanical strain regulates the development of engineered smooth muscle tissue. *Nat Biotechnol* 1999;17:979–83.
- [32] Huang CY, Hagar KL, Frost LE, Sun Y, Cheung HS. Effects of cyclic compressive loading on chondrogenesis of rabbit bone-marrow derived mesenchymal stem cells. *Stem Cells* 2004;22:313–23.
- [33] Mantero S, Sadr N, Riboldi SA, Lorenzoni S, Montevocchi FM. A new electro-mechanical bioreactor for soft tissue engineering. *JABB* 2007;5:107–16.
- [34] Flanagan TC, Cornelissen C, Koch S, Tschoeke B, Sachweh JS, Schmitz-Rode T, et al. The in vitro development of autologous fibrin-based tissue-engineered heart valves through optimised dynamic conditioning. *Biomaterials* 2007;28:3388–97.
- [35] Ritchie AC, Wijaya S, Ong WF, Zhong SP, Chian KS. Dependence of alignment direction on magnitude of strain in esophageal smooth muscle cells. *Biotechnol Bioeng* 2009;102:1703–11.
- [36] Janssen FW, Oostra J, Oorschot A, van Blitterswijk CA. A perfusion bioreactor system capable of producing clinically relevant volumes of tissue-engineered bone: in vivo bone formation showing proof of concept. *Biomaterials* 2006;27:315–23.
- [37] Radisic M, Deen W, Langer R, Vunjak-Novakovic G. Mathematical model of oxygen distribution in engineered cardiac tissue with parallel channel array perfused with culture medium containing oxygen carriers. *Am J Physiol Heart Circ Physiol* 2005;288:H1278–89.
- [38] Botchwey EA, Dupree MA, Pollack SR, Levine EM, Laurencin CT. Tissue engineered bone: measurement of nutrient transport in three-dimensional matrices. *J Biomed Mater Res A* 2003;67:357–67.
- [39] Zhao F, Pathi P, Grayson W, Xing Q, Locke BR, Ma T. Effects of oxygen transport on 3-D human mesenchymal stem cell metabolic activity in perfusion and static cultures: experiments and mathematical model. *Biotechnol Prog* 2005;21:1269–80.
- [40] Williams KA, Saini S, Wick TM. Computational fluid dynamics modeling of steady-state momentum and mass transport in a bioreactor for cartilage tissue engineering. *Biotechnol Prog* 2002;18:951–63.
- [41] Sengers BG, van Donkelaar CC, Oomens CW, Baaijens FP. Computational study of culture conditions and nutrient supply in cartilage tissue engineering. *Biotechnol Prog* 2005;21:1252–61.
- [42] Zhou S, Cui Z, Urban JP. Nutrient gradients in engineered cartilage: metabolic kinetics measurement and mass transfer modeling. *Biotechnol Bioeng* 2008;101(2):408–21.